REPORT DOCUMENTATION PAGE

Form Approved
OMB No. 0704-0188

1. REPORT DATE *(DD-MM-YYYY)*	2. REPORT TYPE	3. DATES COVERED *(From - To)*
11-18-2007	FINAL	Aug 1, 2004 to July 31, 2005

4. TITLE AND SUBTITLE
Cohesive Zone Approach to Multiscale Modeling of Nanotube Reinforced Composites

5a. CONTRACT NUMBER

5b. GRANT NUMBER
FA9550-04-1-0202

5c. PROGRAM ELEMENT NUMBER

6. AUTHOR(S)
Dr. Namas Chandra (PI)

5d. PROJECT NUMBER
37-1906-041 (FAMU 37099)

5e. TASK NUMBER

5f. WORK UNIT NUMBER

7. PERFORMING ORGANIZATION NAME(S) AND ADDRESS(ES)
Florida A&M University

8. PERFORMING ORGANIZATION REPORT NUMBER

9. SPONSORING / MONITORING AGENCY NAME(S) AND ADDRESS(ES)
AFOSR/NA
110 Duncan Avenue B115
Bolling AFB DC 20322-8050
Dr Byung Lee/NA

10. SPONSOR/MONITOR'S ACRONYM(S)

11. SPONSOR/MONITOR'S REPORT NUMBER(S)

12. DISTRIBUTION / AVAILABILITY STATEMENT
Unlimited

AFRL-SR-AR-TR-07-0436

13. SUPPLEMENTARY NOTES

14. ABSTRACT

This one year effort demonstrated that cohesive zone model can be adapted within a multi-scale approach to study the fracture behavior of carbon-nanotube (CNT) based polymer based composites. Some of the fundamental cohesive zone parameters like traction and displacement were computed using molecular dynamics and the results used in a non-linear finite element method to study the fracture characteristics of the CNT based composites. A new type of cohesive zone finite element was developed, and the element showed both numerical stability and accuracy. It was clearly shown using the developed method that unless the interface strength and fracture characteristics are properly controlled, the full capability of CNTs in composites could not be exploited. For example, simple carbon nano-fibers (a few micron in diameter) will outperform CNT based composites, if the former has better interface thermo-mechanical properties than the latter. Controlling atomic scale interfaces is however much more difficult and follow up work showed novel neutron bombardment and selective defect creation can achieve this. The present work paved way for breakthroughs in processing.

15. SUBJECT TERMS

16. SECURITY CLASSIFICATION OF:			17. LIMITATION OF ABSTRACT	18. NUMBER OF PAGES	19a. NAME OF RESPONSIBLE PERSON
a. REPORT	b. ABSTRACT	c. THIS PAGE			19b. TELEPHONE NUMBER *(include area code)*

Final Report Documentation sheet (SF 298)

Cohesive Zone Approach to Multiscale Modeling of Nanotube Reinforced Composites

PI: Namas Chandra

AFOSR number FA9550-04-1-0202

FAMU Project 37099 (37-1906-041)

Final Report

Cohesive Zone Approach to Multiscale Modeling of Nanotube Reinforced Composites

Executive Summary

As a part of the project, a number of scientific advances were made. Though this project covered funding only one year, it provided the necessary background material for advancing the state of the art on cohesive zone model. One of the difficulties in cohesive zone model is that the model parameters cannot be accurately evaluated using experiments. Molecular dynamics provided that data.

ABSTRACT

In order to fully harness the outstanding mechanical properties of carbon nanotubes (CNT) as fiber reinforcements, it is essential to understand the nature of load transfer in the fiber matrix interfacial region of CNT based composites. With controlled experimentation on nanoscale interfaces far-off, molecular dynamics (MD) is evolving as the primary method to model these systems and processes. While MD is capable of simulating atomistic behavior in a deterministic manner, the extremely small length and time scales modeled by MD necessitate multiscale approaches. To study the atomic scale interface effects on composite behavior, we herein develop a hierarchical multiscale methodology linking molecular dynamics and finite element method through atomically informed cohesive zone model parameters to represent interfaces. Motivated by the successful application of pullout tests in conventional composites, we simulate fiber pullout tests of carbon nanotubes in a given matrix using MD. The results of the pullout simulations are then used to evaluate cohesive zone model parameters. These cohesive zone models (CZM) are then used in a finite element setting to study the macroscopic mechanical response of the composites. Thus, the method suggested explicitly accounts for the behavior of nanoscale interfaces existing between the matrix and CNT. The

developed methodology is used to study the effect of interface strength on stiffness of the CNT based composite.

1. Introduction

Carbon nanotubes possess excellent combination of mechanical and thermal properties with high aspect ratio. Stiffness of CNTs measured experimentally [1] and calculated from simulations [2] is of the order of 1000 GPa, while the nearest competitive fiber (SiC whiskers) has utmost 400 GPa stiffness [3]. CNTs have tensile strength of about 150 GPa [4]. The range of elastic deformation and fracture strain are also extremely high [5,6]. In addition, the typical length of CNTs is of the order of a few microns while the diameters range from less than nanometer (for single wall nanotubes) to about 30 nm (for multiwall nanotubes) [7,8] that correspond to an aspect ratio around 1000. This combination of mechanical properties has raised the great possibility of obtaining super-strong and stiff composites with CNTs as reinforcements. Further, the excellent electrical and optical properties of CNTs facilitate development of many multifunctional products [9]. Bulk composites and thin films of CNT based composites with a variety of polymer matrices such as polystyrene, PMMA, Polyurethane, PPA, epoxy and PmPv are being fabricated by a host of researchers [8, 10-14]. In addition, metallic and ceramic materials such as Cu, Al, Ti, SiO_2 and Al_2O_3 have also been used as matrices [15-19] with CNTs as reinforcements.

Good properties of fibers do not necessarily translate into good properties of composites. There are several issues pertaining to alignment, dispersion and load transfer which have to be optimized in order to achieve the possible high strength and stiffness in the composites. This is especially true when the reinforcing elements are in the

nanometer dimension as in CNTs. It is well established through a number of years of research in conventional composites that interface strength is a critical parameter in controlling the load transfer between fiber and matrix, and forms the key issue addressed in this work.

There are conflicting observations in the existing literature regarding the nature of interfacial bonding in CNT based composites. The nanometer length scale of CNTs renders controlled experimentation to measure the interfacial strength extremely difficult, if not impossible. As a result, most of the observations have been extrapolations based on microstructural characterization and bulk property measurement. Several researchers have observed evidence for load transfer based on microscopic and spectroscopic observations [8, 10, 20, 21]. Wagner and coworkers [11] report a high value of interface strength of 500 MPa based on fragmentation tests in urethane - CNT composites. Cooper and coworkers [22] report variation of interface strength in the range of 30-300 MPa based on CNT pullout using scanning probe microscope. On the contrary, there are reports of low interfacial load transfer, for e.g. Schaddler and coworkers [23] use Raman spectroscopy to infer low load transfer between concentric tubes in multiwall nanotubes in epoxy matrix. Similarly, Ajayan and coworkers [24] observe low load transfer in CNT ropes. Most importantly, the measured values of mechanical properties of CNT based composites reported by various researchers are much lower than those predicted by theoretical models [25]. For example, Andrews and coworkers [12] report normalized Young's modulus (stiffness of composite/stiffness of matrix) values in the range of 1.2-2.5 for polystyrene matrix reinforced with 2.5-25 volume % CNT. The comparable theoretical maxima and minima based on parallel and series models are in the range of 14

to 140 and 1.03 to 1.33 respectively. Parallel model corresponds to a perfectly aligned reinforcement with perfect bonding and thus represents true upper bound. Series model is the case when the alignment of all reinforcements are normal to the load, but still perfect bonding and represents a possible lower bound. An intermediate value is obtained if either the reinforcements are randomly aligned and/or the interfacial bonding is less than perfect. As the experimental values are closer to the lower bound, one of the likely reasons is the lack of adequate bond strength given that the alignment is possibly random. Thus, we have a practical reason to understand the CNT-matrix interfaces in these classes of composites.

The purpose of the paper is two fold. First, we establish the fact that interface properties at nanoscale can be significantly improved by enhancing the bond strength between the matrix and CNTs by chemical attachments. We show that this is possible by conducting simulations of pullout tests on a single CNT fiber embedded in a matrix using molecular dynamics. Second, we intend to show that these enhanced interfacial properties at the atomic level translate into substantial increase in the value of composite stiffness at the macro level. This entails development of a multiscale model with FEM modeling the macroscopic continuum, while MD simulates the nanoscale interfaces with atomically informed cohesive zone parameters providing the necessary coupling between MD and FEM.

It should be noted that there are a plethora of approaches in the general area of multiscale modeling concerning two different length scales. We focus our attention only on cases where the smaller length scale is at atomistic level (described by atomic simulations) and the larger length scale is at macroscopic level (described by continuum

concepts). The difficulty encountered in this class of problems is that while atomistic regime is conceived as discrete set of atoms (e.g. modeled by molecular dynamics/statics), continuum methodologies assume the presence of differentiable displacement field with no specific assumptions on the underlying physical matter that causes the said motion.

Many multiscale methods such as quasicontinuum method [26], coarse grained molecular dynamics (CGMD) [27] and hand shaking methods [28] employ intense atomic calculations near the core of atomic scale inhomogeneity and use continuum-based solutions in the homogenously deforming regions. The two regions are linked by various methods. Quasicontinuum invokes Cauchy-Born rule in the continuum regime while CGMD employs statistical averages of atomistic variables. In the handshaking methods kinematic restraints are applied at the boundary of the two regimes.

In addition to above multiscale methods, continuum methods have been applied to study CNTs and CNT based composites, which are essentially nanoscale systems. For example, Yakobson [5] has shown that predictions of continuum shell theories are compatible with atomic simulation results of deformation of nanotubes. There have been attempts to model the elastic behavior of nanotubes using continuum techniques (e.g. [29]). Li and Chou [30] model nanotubes as atomic trusses with stiffness having all the components of covalent bonds (angle dependence, torsion etc). Wagner and coworkers [11] have used Kelly-Tyson model and experimental results to obtain interfacial strength in urethane matrix nanotube composite. Throntenson and coworkers [31] use micromechanistic model to obtain composite effective properties. Fisher and coworkers

[32] have incorporated nanotube waviness into micromechanics model of nanotube composites. These approaches assume perfect bonding at CNT-Matrix interface.

The difference between atomic simulations and continuum methods is with respect to both length and time scales. While the elegance and advantages of unified multiscale models such as CGMD and quasicontinuum are undeniable, their application is constrained due to the disparate time scales of the underlying processes occurring at the different length scales. One approach to counter this problem is by hierarchical multiscale modeling in which the information of atomic simulations is processed and fed into continuum models. In this paper, such a hierarchical multiscale model to address the problem of interfaces in nanotube-based composites is presented.

We use molecular dynamics simulations to simulate CNT pullout test from polymer matrix. The interface is modeled as hydrocarbon chemical attachments bonded to both matrix and fiber. These simulations are used to obtain the constitutive response of the interface in the form of traction-displacement plot for cohesive zone model. This atomically informed CZM is used in finite element framework to study the constitutive response of the composite, thus traversing across the length scale from nano to macro scales.

Because of the hierarchical approach, we can examine various factors at atomic scale, which affect the form and magnitude of parameters that are passed on to continuum simulations. Since CZM is central to our model, section 2 explores how interfaces are represented in both continuum and atomic scales. Section 3 presents the atomic simulations of pullout test and explains the method of extracting the CZM properties

from MD simulations. Section 4 discusses the application of the multiscale model to the problem of determining the stiffness of the composite.

2. Problem Formulation

Interface in general can be defined as a region that separates two distinct bodies. The bodies in question may be of same material (e.g. crystals with different orientation) or different materials (as in the case of composite materials). The bodies may react differently to thermomechanical, electromagnetic or any other externally applied stimuli; hence, interface can be more practically described as a region separating two bodies with different constitutive response. Interfaces have been modeled as either continuous or discrete systems based on the problem of interest and the length scale. In the case of interfaces between two phases of composite material, the primary interest is to study the load transfer between the phases across the interface. For such problems, finite element based methods are adequate provided the general constitutive response of the interface region is known. Several such continuum methods have been developed; for example, interface region has been modeled as a thin surface separated by springs [33-35] and as narrow continuum with graded mechanical properties [36]. Another method consists of incorporating the interface within continuum description based on cohesive zone models [37, 38].

Interfaces can also be perceived as two-dimensional defects in an otherwise homogenous atomic structure. This would be a high-energy region with many processes related to atomic structural changes and chemical reactions occurring in a narrow region. For example, there is evidence of formation of series of carbides in the interfaces of SiC-

Ti metal matrix composites [39]. Atomic simulation can be employed to obtain the constitutive law required for continuum formulation of interface incorporating the structural and chemical changes occurring at the interfaces. We now discuss the representation of interfaces employing continuum based cohesive zone models as well as discrete molecular dynamics approach.

Continuum model for interface

Consider two bodies Ω_1 and Ω_2 separated by an interfacial region γ (figure 1). The two bodies can be considered as matrix and fiber of the composite material. In order to study the load transfer between the bodies Ω_1 and Ω_2, we need to subject the bodies to a relative motion with respect to each other. Let the system be subjected to external displacement (or traction) as shown in figure 1 (a). Under the action of external load a material point initially at $\mathbf{X}$ in either of bodies Ω_1 or Ω_2 moves to a new location $\mathbf{x}$. This transformation can be described by any of the strain measures, for instance deformation gradient can be expressed as:

$$\mathbf{F} = \frac{d\mathbf{x}}{d\mathbf{X}} \tag{1}$$

The kinematic measure can be related to its kinetic conjugate through the appropriate constitutive relation as shown below

$$\mathbf{P} = \mathbf{CF} \tag{2}$$

where, $\mathbf{P}$ is the first Piola-Kirchoff stress and $\mathbf{C}$ represents the linear or nonlinear stiffness of the material. Using this constitutive relation in the equilibrium relation we obtain

$$\frac{\partial}{\partial \mathbf{x}}(\mathbf{CF}) + \mathbf{f} = 0 \tag{3}$$

This equation can be solved with appropriate boundary conditions to completely describe the bodies Ω_1 and Ω_2. Now, consider the interface region γ. A point P on the interface lies on the surface described by the unit normal **N.** If the material deforms and fractures along the interface as shown in figure 1(b), two new surfaces are created (represented by unit normals $\mathbf{n_1}$ and $\mathbf{n_2}$). The material point, which was at P in the initial configuration, now corresponds to two points P1 and P2. This results in the loss of one to one correspondence between the two (undeformed and fractured) configurations thus violating the fundamental tenets of continuity.

One of the methods to counter this problem is to use cohesive zone models. We assume that the interface is a different continuous material with an independent constitutive relation. The constitutive relation for the interface material is given as a displacement dependent potential i.e. the measure of energy required to extend the interface material by a certain relative displacement δ between the two originally mating surfaces. The resulting tractions on the interface can be expressed as:

$$if \left|\boldsymbol{\delta}\right| < \left|\boldsymbol{\delta}_{sep}\right|, \quad \boldsymbol{\tau} = \boldsymbol{\sigma}.\mathbf{n} = f\left(\boldsymbol{\delta}\right) \tag{4}$$

$$if \left|\boldsymbol{\delta}\right| > \left|\boldsymbol{\delta}_{sep}\right|, \quad \boldsymbol{\tau} = \boldsymbol{\sigma}.\mathbf{n} = 0 \tag{5}$$

Now the point P can be considered as two identical points $P1^i$ and $P2^i$, which after deformation (or fracture) move to the new points P1 and P2. Through this method, we can incorporate the interface deformation and fracture into the purview of continuum mechanics. This is the advantage of CZM over ad hoc numerical schemes such as springs.

Cohesive zone model was first proposed by Barrenblatt [40] and subsequently extended to ductile and quasi-brittle materials by Dugdale [41] and Hillerborg [42] respectively. In

the recent years, CZM has been applied to a number of systems to solve numerous problems of fracture and interfaces in different materials. Different models have been used to represent the traction-displacement constitutive relations and are tabulated by Shet and Chandra [38]. The models differ in the shape and the points of inflexion *i.e.* the maximum load and separation distance. Chandra and coworkers [37] emphasize that the apart from maximum stress and separation distance, the shape of traction –displacement curve is also an important parameter in accurately representing the material behavior.

Atomistic model for interface

We now look at the atomic description of the interface problem discussed earlier using molecular dynamics. Molecular dynamics involves numerical solution of Newton's laws of motion for a set of atoms. Here we solve for the atomic degrees of freedom i.e. the positions and velocities, unlike in continuum where the solution is for structural degree of freedom. Molecular dynamics needs specification of the geometry of the system (initial positions and velocities of atoms) and an energy function that describes the interaction between the atoms. For a set of N atoms interacting through a potential $\phi(r_{ij})$, the interatomic force on atom i due to atom j ($\mathbf{f}_{ij}$) can be obtained as:

$$\mathbf{f}_{ij} = \frac{\partial \boldsymbol{\phi}(r_{ij})}{\partial r_{ij}} \frac{\mathbf{r}_{ij}}{r_{ij}} \tag{6}$$

The total force experienced by atom i is the sum of forces due to the different particles it interacts and the forces external to the system.

$$\mathbf{f}_i = \sum_j \mathbf{f}_{ij} + \mathbf{f}^o \tag{7}$$

The system evolves in time and reaches equilibrium and the physical and structural properties and the properties of interest are calculated as statistical averages.

Consider the same bodies Ω_1 and Ω_2 separated by the interfacial region γ, but the bodies Ω_1, Ω_2 and γ are now composed of discrete atoms interacting based on an interatomic potential. In this case, the motion of individual atoms and the forces acting between them is the basis for load transfer. Interestingly, the concept of surface is not clearly defined in the discrete description; an envelope of all atoms bounding a predefined region can be considered as surface. The interface γ can be considered a region bounded by two such surfaces (χ_1 and χ_2 in figure 2).

In order to displace the two bodies (Ω_1 and Ω_2) with respect to each other, a fixed displacement (or force) is applied on a set of atoms at the end of body Ω_2 (region ω in figure 2a) and the effect is transmitted through the system. For example, if the atom 1 (see figure 2b) is subject to external displacement **u,** there is a change in the relative position vectors $\mathbf{r}_{1j}$ as well as the bond angles θ_{1j} with all the j atoms it interacts. Correspondingly, there the force ($\mathbf{f}_{1j}$) experienced by the neighboring atoms changes and this effect propagates from Ω_1 to Ω_2 through the interface region γ.

The magnitude of the forces between the atoms in the interface region γ determines the extent to which the external load applied on body Ω_2 is transferred to body Ω_1. These forces are directly dependent on the bond strength between the atoms in the interface region. If the bond strength of atoms in the interface region is high, this implies that a small separation between the atoms from equilibrium bond length requires a high energy input, correspondingly the forces between atoms that are responsible for the load transfer will be high. On the contrary, if the bond strength in the interface region is low (for example, Vanderwall's interactions) the force which is transferred to Ω_1 form Ω_2 will be low resulting in a low load transfer.

In order to obtain the traction-displacement (τ-δ) relation for CZM from molecular dynamics, we need to calculate the stress transmitted to the matrix (Ω_1) for the applied displacement. This is the traction experienced on surface χ_2 (see figure 2) between the interface and matrix. There are various definitions of stress in MD and a discussion regarding their applicability to CNTs is discussed by Chandra and coworkers [43]. Traction experienced across the surface can be obtained using Yip's stress below:

$$\sigma_{\alpha\beta} = \frac{1}{A}\left[\frac{1}{2}\sum_i \frac{m^i v_\alpha^i}{\Delta t} - \sum_i \sum_j \frac{\partial V}{\partial r^{ij}} \frac{r_\alpha^{ij} r_\beta^{ij}}{\left|\bar{r}_\beta^{ij}\right|}\right] \tag{8}$$

Where α, β correspond to x, y and z directions, *i, j* are atom indices, A is the area of the plane and V is the interatomic potential. m, v and Δt are the mass velocity and time interval. The first term corresponds to momentum flux through the area A and the second term is total force per unit area.

Since we are interested only on the stress transmitted to the matrix, we need not model the matrix explicitly. Consider the situation as shown in figure 2c where the matrix is not explicitly modeled, instead the atoms on the surface χ_2 are fixed. The reaction force experienced by the fixed atoms would be the force transmitted to the matrix (Ω_1). The stress in equation (8) above can now be calculated as the total reaction force divided by the corresponding area.

The multiscale model proposed can be summarized as follows. Consider the situation when Ω_1 and Ω_2 can be adequately modeled by continuum methods connected by the interfacial region γ demanding atomistic description modeled by molecular dynamics. The interfacial region can be represented in continuum as a surface experiencing traction

τ with displacement δ. This traction can be determined by molecular dynamics simulations as the force experienced on the surface separating Ω_2 and γ per unit area. It must be noted that this is a one way coupling going from MD to continuum and not vice versa. However, all nonlinearities arising out of geometry, material or boundary conditions at the continuum level can be handled by the model.

Concerning the problem of CNT based composites studied in this paper, the interfacial region between CNT and matrix is modeled as hydrocarbon groups chemically bonded to the CNT. Chemical bonding between matrix and CNTs is perceived to improve strength immensely; Frankland and coworkers [44] have demonstrated the effect of cross-linking using molecular dynamics simulation of CNTs in a polymer matrix. Wagner and coworkers [11,45] report 2-2 cycloaddition reaction as a possible reason for high interfacial strength in polyurethane-CNT composites. Jia and coworkers [10] observe that use of AIBN initiator causes chemical bonding between PMMA matrix and CNT. In addition, there have been a number of investigations of surface modification of nanotubes leading to addition of various functional groups like esters, amides, hydrocarbons, hydrogen, fluorine etc to CNT [46, 47]. Based on MD simulations Namilae and coworkers [48] have observed that the mechanical properties of functionalized CNTs are comparable to that of defect free CNTs. The results of atomic simulation are now discussed.

3. Atomic Simulation of CNT Pullout Tests

Evaluation of interfacial properties in composite materials is typically done using single fiber pullout and pushout tests. The output of these tests is the force required for debonding the fiber from matrix and the shear-stress distribution along the interface. In

addition to experimental investigations, there have been a number of finite element based numerical investigations of pullout and pushout tests to understand the thermomechanical behavior of interfaces. In the case of CNT reinforced composites, experimental application of mechanical loads on single fibers is extremely difficult because of the nanometer size of fibers. There has been only one experimental determination of interface strength by pullout test using scanning probe microscope [22]. Conducting these tests on a regular basis in different materials for different boundary conditions is beyond the current experimental capabilities; hence, molecular dynamics simulations become a natural choice for studying the interface behavior. Lordi and Yao [49], Liao and coworkers [50] have simulated pullout tests with non-bonded interactions using molecular statics, but there has not been any detailed investigation in the case of bonded interactions. We consider the situation where matrix and nanotube are chemically bounded by hydrocarbons chains.

Tersoff-Brenner potential [51] is used to calculate C-C and C-H chemical interactions. The potential has coordination dependant terms, which enable modeling of bond conjugation in carbon, and has been used by numerous investigators to study processes such as deformation of carbon nanotubes [5, 6], and various surface chemical reactions in carbon-hydrogen systems [52]. Linear hydrocarbons modify the planar SP2 configuration of CNT to tetrahedral SP3 bond with a pi orbital on the CNT surface. This change in bonding and increase in bond length to 1.54 $\mathring{A}$ is accurately represented using Tersoff-Brenner potential.

The boundary conditions applied for the pullout test simulation are shown schematically in the figure 3. The corner atoms of the hydrocarbon attachments are fixed indicating that they are connected to matrix at those locations. Displacement of 0.05 $\mathring{A}$ is applied to the atoms at one end of the nanotube, about 15 $\mathring{A}$ in length in order to simulate the effect of pullout. Following each displacement, the system was equilibrated for 1500 time steps of 0.2 fs duration. The simulations were carried out until some of the hydrocarbon chains fail. Typically, simulations lasted for 500000-800000 time steps. Variations in the length and density (number per unit area) of chemical attachments were investigated for a (10,10) CNT 122 $\mathring{A}$ in length. The reaction force on the fixed atoms is monitored throughout the simulation and is averaged over 100 time steps before applying the next set of displacements.

Figure 4 shows typical force vs. displacement for any hydrocarbon attachment. The force in the figure is the average reaction force experienced by the fixed atom in the direction along the length of nanotube and corresponds to shear. Displacement is calculated as the change in the position experienced by the atom that is initially attached to the CNT. Though there are statistical variations for different chemical attachments, the general shape of the force displacement plot is as shown in figure 4.

The initial region of curve is flat (parallel to displacement axis) marked as region (a). This region corresponds to stretching of the hydrocarbon attachment. The flat region shows that there is minimal load transfer in this portion of curve and is similar to the mechanical analogue of a loose string becoming taut. The length of this flat portion is directly dependant on the length of hydrocarbon chain i.e. the flat region is longer for

hydrocarbon chains with four and five carbon atoms than with two carbon atoms. After this flat region, there is a gradual increase in the reaction force corresponding to region (b) of the curve. In this part, the carbon chain contributes to the load transfer. Though there are statistical variations from plot to plot, the typical force experienced in this portion of the curve is about 3eV/$\mathring{A}$ (4.8×10^{-3} μN). This value of force is very small but it must be noted that the area on which this force acts is of the order of angstroms; consequently, the resulting shear stress is very high. Region (c) of the plot as shown consists of fluctuations in the reaction force. This is due to an interesting behavior of bond separation and rejoining with adjacent atoms; when the separation occurs there is a sudden drop in force but this is followed by rejoining of the hydrocarbon chain with adjacent atom of the CNT. After the jagged region, there is a sudden increase in reaction force as shown in region (d) of the figure followed by total failure. The force at which the failure occurs is about 6eV/$\mathring{A}$ ($\sim 10^{-2}$ μN). This is the force required to break one chemical attachment; the overall force required to break all the chemical attachments is much higher and is sum of all individual reaction forces.

The area under the force-displacement curve denotes the energy required for detaching of the hydrocarbon group from CNT. Calculations based on molecular statics indicate that the energy required for separation is of the order of 3 eV. However, the area under the force displacement curve is much greater and is about 20±4 eV for various attachments. This shows that the dynamic process of nanotube pullout requires much higher energy than that predicted based on statics. Energy of 3 eV is associated with each time the bond is broken, as this process is repeated number of times for each chemical attachment the total energy consumed in the separation process is much higher.

Different cases were considered with varying number of chemical attachments. For the (10,10) CNT studied here, there are 85 chemical attachments if one chemical attachment is attached per repeat unit of the CNT excluding the end of CNT that is subject to displacement. Different number of chemical attachments 85, 45, 20, 10 and 5 are attached at circumferentially random and cylindrically equidistant locations and pullout tests are simulated with all the other variables such as temperature and displacement rate being constant. The general shape of force-displacement curve remains similar to that shown in figure 4. The values of points of inflexion also remain similar within statistical variation, but there is a tendency for extended debonding and rebonding region when the density of chemical attachments is lowered. This could be ascribed to the fact that the distribution of load is uniform when fewer hydrocarbon chains are attached to the CNT.

The debonding-rebonding behavior observed in pullout test is unique to nanoscale and is generally not observed in conventional composites at macroscopic scale. Macroscopic fracture is generally considered irreversible, i.e., the energy required in creation of new surface during fracture is not equal to energy required to join two surfaces and heal the damage. At atomic scale, fracture is defined by breaking of chemical bonds. The energy required to break two bonds is exactly equal to the energy released to join the same two atoms to form chemical bond. Whether two atoms will join to form a chemical bond is determined based on the distance between the atoms and the kinetics of the process. This phenomenon is not entirely new; for example, similar observations have been made during atomic simulations of stick slip friction and that of metal cutting processes. Zhang and Tanaka [53] have performed simulations of friction

on copper surfaces; they observe variation of frictional force in oscillatory manner similar to that of reaction force observed in our simulations. Further, the frictional force during rolling of nanotube on graphene sheet produces similar periodic variations [54]. However, significance of this phenomenon is increased here since it affects the load transfer considerably.

Traction displacement relation for nanoscale interfaces

We now proceed to obtain the interface constitutive relation based on the above discussed atomic simulation results. An interesting aspect of using CZM to model the interfaces is that, all the micro mechanical details occurring during the load transfer and failure are taken into account in the traction displacement relation. For example, in conventional fiber composites various micromechanisms such as crack deflection, crack closure, fiber bridging, inelastic dissipation etc act simultaneously and are represented in an average sense in the extrinsic and intrinsic regions of the τ-δ relation. In the case of CNT based composites, various mechanisms such as chemical bonding, bond breaking and joining, Vanderwall's interactions, nanotube curvature etc may affect the load transfer. By using atomic simulations to determine the τ-δ relation, we include some of these mechanisms into the continuum formulations.

There is an additional complexity involved in obtaining cohesive zone information from atomic simulations. Because of discrete numerical implementation of finite element method, a given discretized element experiences the constitutive response as a single unit (albeit based on an interpolation) according to the traction displacement response. The element dimensions can be refined to the order of few nanometers, but it would still physically correspond to a large number of functional group attachments. We

need some way to homogenize the force displacement relations shown in the preceding section to obtain the traction displacement plots that are on the scale of element. Simple averaging over all the chemical chains will not serve this purpose since the effect of length and density would be ignored. In other words, if only few chemical attachments near the loading end take up most of the load, then the traction displacement plot obtained by averaging over the entire length of CNT would give an erroneous underestimation.

Figure 5 shows variation of reaction forces for specific atoms in the hydrocarbon attachments across the length of (10,10) CNT with 85 attachments. It can be observed that the variation of force occurs in a sequential manner. We can divide the typical force displacement into various parts initial loading b, debonding-rebonding region c, maximum loading region d, and failure denoted by e (See figure 4). Typically, the force displacement plots of each chemical attachment go through these regions in a self-similar manner until they fail. As expected the chemical attachments near the loading region reach the peak stress and fail sooner than the chemical attachments away from the loading end. Once the chemical attachments detach completely from the CNT, it fails to take up any more load; thus, the peak stress region moves progressively from the loading end to the other end. Figure 6 schematically depicts this process. The various shades of gray in the figure 6 (b-e) represent the different stages of force-displacement plot, from no loading to full loading and again no load moving away from the loading end. There is a gradual progression of the fractured region. For example, Figure 5(a) at 20 and 24 ps shows atoms near the loading end taking up load. In figure 5(b) the chemical attachments near the loading end are in debonding-rebonding phase while additional chemical

attachments take up load (region a). In the figures 5 (c) and (d) the chemical attachments near the loading end reach maximum load and failure (region d). The maximum load region moves away from the loading end as shown in figures 5 (e) and (f). At any point of time about forty chemical attachments only take load and others have either failed or yet to be loaded. Based on above observations, we have taken the average of these plots with applied displacement for forty chemical attachments and divided by corresponding area to obtain the traction displacement plots. In the case of lower number of chemical attachments, we observe that all the chemical attachments take similar load at any given time and the corresponding area is used for the traction calculation. The traction-displacement plots for use in cohesive zone are obtained by extrapolating figures to complete failure as shown schematically in the figure 7.

An interesting observation of this investigation is the very high interfacial strength obtained when there is chemical bonding between matrix and CNT. For high degree of chemical bonding (85 chemical attachments) we obtain interfacial strength as high as 5 GPa which is about two orders of magnitude higher than that typically observed in conventional carbon fiber reinforced polymeric composites [55]. In the case of five hydrocarbon attachments distributed over 122 $\mathring{A}$ we obtain an interfacial peak strength of 500 MPa. It is interesting to note that experimental measurements of interfacial strength by Wagner et. al. [11] and by Cooper et. al. [22] are of the same order. Further, Wagner and coworkers indicate that this high value might be due to chemical interaction between CNTs and urethane matrix. We obtain only a value of about 50 MPa of strength when number of chemical attachments in 200 $\mathring{A}$ length CNT is only three. These

observations indicate the strength of the interface can be altered by two orders of magnitude by altering the density of chemical attachments.

4. Cohesive Zone Modeling of Nanoscale Interfaces

We can now apply the atomically (MD) informed traction displacement plots in finite element simulations of CNT reinforced composites. In order to demonstrate the effectiveness of the multiscale model we study the elastic behavior of the composite and the effect of interfacial strength on the stiffness. It is a common practice to evaluate the mechanical behavior of conventional composites using representative volume element (RVE). Because of their ability to fill space, square or hexagonal RVEs are popular in formulations. Cylindrical RVEs using axisymmetric formulations require less computational effort.

The finite element mesh and the boundary conditions are as shown in the figure 8. Axisymmetric four node cohesive zone elements with zero initial thickness in the direction normal to the interface are used to model the interface behavior. The traction displacement plots discussed in the previous section form the constitutive behavior of the interface while the matrix and the nanotubes are modeled as continuum with appropriate elastic properties. Four node axisymmetric elements are employed to descretize both matrix and CNT. The models typically consist of 1000 elements (variation for different fiber content) and the interface consists of 93 cohesive zone elements. CNT length is assumed to be 450 A and diameter of 20 A. In these computations CNT is considered as solid cylinder; this can be justified by assuming a multiwalled nanotube with innermost tube of very small radius (for e.g. (5,0) nanotube). Both the matrix and CNT are assumed continuous media exhibiting homogenous linear elastic isotropic behavior with a given

Young's modulus and Poisson's ratio. Young's modulus of 1000 GPa and Poisson's ratio of 0.3 are employed for the nanotube. The general-purpose commercial code ABAQUS [56] is employed to carry out the analysis. The cohesive element model is input as a user-defined element subroutine UEL into ABAQUS. Parametric studies for different interfacial strengths to understand the effect of interfacial strength on the stiffness and load transfer of composite.

Effect of interface strength

Two extreme cases of load transfer occur either when the interfacial stress transfer is perfect or when there is zero load transfer between the matrix and fiber. In terms of CZM, these two cases would correspond to infinite and zero peak traction respectively. In the case of zero interfacial traction, the composite elastic properties trivially become equal to that of matrix material as no load transfer occurs. The stiffness of the composite progressively increases as the peak traction of CZM increases. For very high value of peak stress the load transfer should be near maximum possible load transfer and correspondingly the elastic modulus of the composite should be near that of ideal interface. This concept is illustrated in figure 9. The figure shows variation of composite elastic modulus with volume percentage CNT for various CZMs described in the earlier section. When the matrix and CNT are connected by a large number of chemical attachments (one per repeat unit of CNT), the interfacial strength is very high and the peak traction is of the order of 5 GPa. This high interfacial strength leads to stiffness values near that of ideal composite with perfectly bonded interface as seen in figure 9.

On the other extreme when the peak traction is 5 MPa (this is a fictitious traction displacement plot and does not correspond any atomic simulation result), the composite

stiffness is close to that of matrix material (denoted by dotted line in figure 9). The more likely values of interfacial peak traction are between 50 and 500 MPa which correspond to 3 bonds per 200 A CNT and 5 bonds for 100 A CNT. In these cases, stiffness of composite is about 80% and 60% of the maximum possible value (perfect interface). This emphasizes the importance of interface load transfer in determining the stiffness of nanotube reinforced composites

Variation of fiber stiffness

Figure 10 shows the variation of composite stiffness for various fibers (different stiffnesses) and interface stiffnesses in epoxy matrix (E=3.5 GPA). Different fiber stiffness values corresponding to those of glass fibers (E=85 GPa), carbon fibers (E=300GPa), SiC whiskers (E=400 GPa) and CNT (E=1000GPa) are used. CNT reinforced composites in general exhibit much higher stiffness than other composites with other reinforcements. To provide a numerical perspective typical values of interfacial strength in polymeric composites are about 50 MPa. It can be observed from the figure that CNT based composites with high degree of chemical attachments have the potential to reach stiffness of about 300 % of that of conventional carbon fiber reinforced composites. This emphasizes the potential properties possible by surface modification of CNTs.

Variation of matrix stiffness

Figure 11 shows the variation of composite stiffness with matrix stiffness for various CZMs. Typical values of elastic moduli for polymeric systems range from 1 GPa to 10 GPa. Four matrix elastic moduli of 1, 3.5, 5 and 10 GPa are considered in this study. The composite stiffness increases with increase in matrix stiffness and decreases with

lowering of interfacial strength as expected. The ratio of composite stiffness to matrix stiffness is higher for matrices with lower stiffness. It can be observed from the figure that low interfacial strength (5 MPa) results in composite with stiffness similar to that of matrix while composite with high interface strength (5GPa) has stiffness close to that of perfect interface. The plot shows that high interface strength is as critical as matrix properties if not more.

5. Summary

Carbon nanotubes, with their unique mechanical properties have great potential as reinforcements in ultra strong and ultra stiff composites. Weak interfaces significantly reduce the ability of CNTs in providing those high levels of reinforcement. Chemical attachments to CNTs can provide high interfacial strength. Summarizing the paper:

- A hierarchical multiscale model is developed to study the mechanics of interfaces in CNT based composites. The model employs atomistically informed cohesive zone traction displacement relations to link the atomic and macroscopic scales.
- Molecular dynamics simulations of CNT pullout tests are performed to quantify the interfacial behavior. The interfaces between CNT and matrix are modeled as hydrocarbon chemical attachments.
- Interfacial strength as high as 5GPa can be obtained by chemically bonding the matrix and CNTs
- Interfacial strength varies as a function of number of chemical attachments per unit surface area, i.e. density of chemical attachments.

- The multiscale model is employed to study the effect of interface strength on the elastic properties of composites. It is found that interfaces significantly alter the elastic response of CNT based composites

Acknowledgements

Authors wish to thank Chandrakanth Shet, Leon van Dommelen and Ashok Srinivasan for useful discussions. Financial support from ARO (Dr Bruce La Mattina) and AFOSR (Dr Les Lee) is gratefully acknowledged.

References

1. M.M.J. Treacy, T.W. Ebbesen and J.M. Gibbson, Exceptionally high Young's modulus observed for individual carbon nanotubes. Nature 381, 678, (1996)
2. D.H. Robertson, D.W. Brenner and J.W. Mintmire. Energetics of nanoscale graphitic tubules, Physical Review B, 45, 12592, (1992)
3. Engineered Materials Handbook, Volume 1, Composites, ASM International, 1987
4. B.G. Demczyk, Y.M. Wang, J. Cumings, M. Hetman, W. Han, A. Zettl and R.O. Ritchie, Direct mechanical measurement of the tensile strength and elastic modulus of multiwalled carbon nanotubes. Materials Science and Engineering A, 334, 173, (2002)
5. B.I. Yakobson, C.J. Brabec and J. Bernholc, Nanomechanics of carbon tubes: Instabilities beyond linear response. Physical Review letters, 76, 2511 (1996)
6. T. Belytschko, S.P. Xiao, G.C. Schatz and R.S. Ruoff, Atomistic simulations of nanotube fracture. Physical Review B 65, 235430 (2002).
7. Z.W. Pan, S. S. Xie, L. Lu, B. H. Chang, L. F. Sun, W. Y. Zhou, G. Wang and D. L.Zhang, Tensile tests of ropes of very long aligned multiwalled carbon nanotubes, Applied Physics Letters, 74(21), 3152 (1999)
8. D. Qian, E. C. Dickey, R. Andrews and T. Rantell, Load transfer and deformation mechanisms in carbon nanotube-polystyrene composites. Applied Physics letters, 76, 2868, (2000)
9. Q. H. Wang, A. A. Setlur, J. M. Lauerhaas, J. Y. Dai, E. W. Seelig and R. P. H. Chang, "A nanotube-based field-emission flat panel display", Applied Physics Letters, 72, 2912 (1998)
10. Z. Jia, Z. Wang, C. Xu, J. Liang, B. Wei, D. Wu and S. Zhu, Study on poly(methly methacrylate)carbon nanotube composites. Materials Science and Engineering A, 271, 395, (1999)
11. H. D. Wagner, O. Lourie, Y. Feldman, and R. Tenne, Stress-induced fragmentation of multiwall carbon nanotubes in a polymer matrix. Applied Physics letters, 72 , 188, (1998)

12. R. Andrews, D. Jacques, M. Minot and T. Rantell, Fabrication of carbon multiwalled nanotube/polymer composites by shear mixing. Macromolecular Materials and Engineering, 287, 395, (2002)
13. M.P. Ajayan, O. Stephan, C. Colliex and D. Trauth, Aligned carbon nanotube arrays formed by cutting a polymer resin-nanotube composite. Science, 265, 1212, (1994)
14. B. McCarthy, J. N. Coleman, R. Czerw, A. B. Dalton, D. L. Caroll and W.J. Blau, Microscopic study of nanotube-conjugated polymer interactions. Synthetic Metals, 121, 1225, (2001)
15. S.R. Dong , J.P. Tu , X.B. Zhang , "An investigation of the sliding wear behavior of Cu-matrix composite reinforced by carbon nanotubes" Materials Science and Engineering A313, 83, (2001)
16. T. Kuzumaki, K. Miyazawa, H. Ichinose and K Ito, "Processing of carbon nanotube reinforced aluminum composite", Journal of materials research, 13, 2445, (1998)
17. T. Kuzumaki, O. Ujiie, H. Ichinose, K. Ito, "Mechanical characteristics and preparation of carbon nanotube fiber-reinforced Ti composite", Advanced Engineering Materials, 2,416, (2000)
18. J. Ning, J. Zhang, Y. Pan and J. Guo, "Fabrication and mechanical properties of SiO2 matrix composites reinforced by carbon nanotube ", Materials Science and Engineering, A357, 392, (2003)
19. R. Kamalakaran, F. Lupo, N. Grobert, D. Lozano-Castello, N.Y. Jin-Phillipp, M. Ruhle, "In-situ formation of carbon nanotubes in an alumina-nanotube composite by spray pyrolysis", Carbon, 41, 2737, (2003)
20. C.A. Cooper, R.J. Young and M. Halsall, "Investigation into the deformation of carbon nanotubes and their composites through the use of Raman spectroscopy", Composites: Part A 32, 401, (2001)
21. J.R. Wood, Q. Zhao and H. D. Wagner, Orientation of carbon nanotubes in polymers and its detection by Raman spectroscopy. Composites: Part A, 32, 391, (2001)
22. C. A. Cooper, S. R. Cohen, A. H. Barber and H. D. Wagner, Detachment of nanotubes from a polymer matrix. Applied Physics Letters, 81, 3873, (2002)
23. L.S. Schadler, S. C. Giannaris and P. M. Ajayan, Load transfer in carbon nanotube epoxy composites. Applied Physics Letters, 73(26), 3842, (1998)
24. P. M. Ajayan, L. S. Schadler, C. Giannaris and A. Rubio, Single-walled carbon nanotube-polymer composites: strength and weakness Advanced Materials, 12,750, (2000)
25. S. Namilae, PhD Dissertation, Florida State University (2004)
26. E. B. Tadmor , R. Philips and M. Ortiz, Quasicontinuum analysis of defects in solids. Philosophical Magazine A, 73, 1529, (1996)
27. R. E. Rudd and J. Q. Broughton, Concurrent Coupling of Length Scales in Solid State Systems. Physica Status Solidi B, 217, 251, (2000)
28. E. Lidorikis, M. E. Bachlechner, R. K. Kalia, A. Nakano, P. Vashishta and G. J. Voyiadjis, Coupling length scales for multiscale atomistics-continuum simulations: Atomistically induced stress distributions in Si/Si3N4 nanopixels. Physical Review letters, 87, 086104, (2001)

29. D. Qian, W.K. Liu, R.S. Ruoff, Mechanics of C60 in Nanotubes. Journal of Physical Chemistry B 105, 10753 (2001).
30. C. Y. Li and T. W. Chou, A structural mechanics approach for the analysis of carbon nanotubes. International Journal of Solids and Structures, 40, 2487, (2003)
31. E.T. Thostenson and T.W. Chou, On the elastic properties of carbon nanotube-based composites: Modeling and characterization, Journal of Physics D, 36, 573, (2003)
32. F.T. Fisher, R. D. Bradshaw and L. C. Brinson, Effects of nanotube waviness on the modulus of nanotube-reinforced polymers, Applied Physics Letters, 80, 4647, (2002)
33. C.R. Ananth and N. Chandra, Numerical modeling of fiber pushout testing metallic ceramic and intermetallic matrix composites - Mechanics of the failure processes. Journal of Composite Materials, 29, 1488, (1995)
34. S. Mukherjee, C.R. Ananth, N. Chandra Effect of residual stresses on the interfacial fracture behavior of metal-matrix composites, Composite Science and Technology, 57, 1501 (1997)
35. N. Chandra, C.R. Ananth, Analysis of interfacial behavior in MMCS and IMCS using thin-slice push-out tests. Composite Science and Technology 54, 87, (1995)
36. G.P. Carman, R.C. Averill, K.L. Reifsnider and J.N. Reddy, Optimization of Fiber Coatings to Minimize Stress-Concentrations In Composite-Materials. Journal of composite materials, 27, 589, (1993)
37. N. Chandra, H. Li, C. Shet, and H. Ghonem, Some issues in the application of cohesive zone models for metal ceramic interfaces. International Journal of Solids and Structures, 39, 2827 (2002)
38. C. Shet and N. Chandra, Analysis of energy balance when using cohesive zone models to simulate fracture processes, Journal of Engineering Materials & Technology, 124, 440, (2002).
39. S. Mukherjee, C.R. Ananth and N. Chandra, "Evaluation of fracture toughness of MMC interfaces using this-slice push out tests", Scripta Materialia, 36,1333, (1997)
40. G.I. Barrenblatt, The formation of equilibrium cracks in brittle fracture. General ideas and hypothesis. Axially-smmetric cracks. Prikl. Matem. I mekham, 23, 434, (1959)
41. D.S. Dugdale, Yielding of steel sheets containing silts. Journal of Mechanics Physics of Solids. 8, 100, (1959)
42. A. Hillerborg, M. Modeer, P. E. Petersson, Analysis of crack formation and crack growth in concrete by means of fracture mechanics and finite elements. Cement Concrete Research, 6, 773, (1976)
43. N. Chandra, S. Namilae, and C. Shet, Local elastic properties of carbon nanotubes in the presence of Stone -Wales defects, Physical Review B, 69, 094101, (2004)
44. S. J. V. Frankland, A. Caglar, D. W. Brenner, and M. Griebel, Molecular Simulation of the Influence of Chemical Cross-Links on the Shear Strength of Carbon Nanotube-Polymer Interfaces. Journal of. Physical Chemistry B, 106, 3046, (2002)

45. O. Lourie and H. Wagner Evidence of stress transfer and formation of fracture clusters in carbon nanotube-based composites, Composites Science and Technology, 59, 975, (1999)
46. Y.P. Sun, K. Fu, Y. Lin and W. Huang, Functionalized carbon nanotubes: Properties and applications. Accounts of Chemical Research 35, 1096,(2002)
47. A. Eitan, K. Jiang, D. Dukes, R. Andrews, and L. S. Schadler, Surface modification of multiwalled carbon nanotubes: Toward the tailoring of the interface in polymer composites. Chemistry of Materials, 15, 3198, (2003)
48. S. Namilae, N. Chandra, and C. Shet, Mechanical behavior of functionalized nanotubes, Chemical Physics Letters, 387,247, (2004)
49. V. Lordi and N. Yao Molecular mechanics of binding in carbon-nanotube-polymer composites. Journal of Materials Research, 15, 2770, (2000)
50. K. Liao and S. Li, Interfacial characteristics of a carbon nanotube-polystyrene composite system. Applied Physics Letters, 79, 4225, (2001)
51. D.W. Brenner, Emperical potential for hydrocarbon for use in simulating the chemical vapor deposition of diamond films. Physical Review B, 42, 9458, (1991)
52. E.R. Williams, G.C. Jones Jr., L. Fang, R.N. Zare, B.J.Garrison, D.W. Brenner, Ion pickup of large, surface-adsorbed molecules - a demonstration of the Eley - Rideal mechanism. Journal of American Chemical Society, 114, 3207, (1992)
53. L. Zhang and H. Tanaka, Towards a deeper understanding of wear and friction on the atomic scale - a molecular dynamics analysis, Wear, 211, 44, (1997)
54. A. Buldum , J.P. Lu, Modeling and simulations of carbon nanotubes and their junctions on surfaces. Applied Surface Science 219, 123(2003)
55. H. D. Wagner, J. Aronhime, and G. Marom, Proc. R. Soc. London, A428, 493 (1990)
56. ABAQUS, 2003 Manual, version 6.3, Habbit, Karlsson & Sorensen Inc. USA.

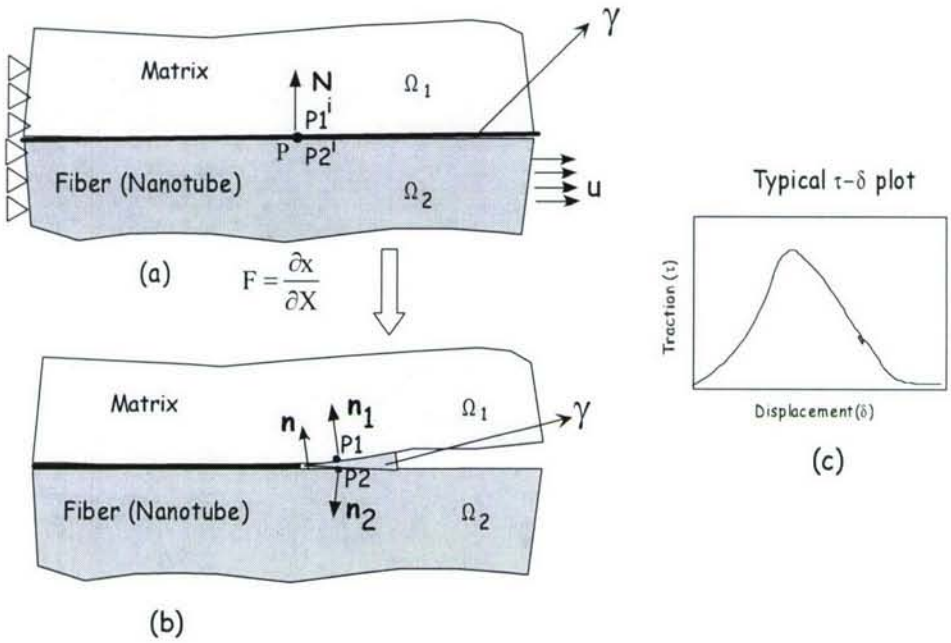

Figure 1. Illustration of Cohesive Zone model for interfaces

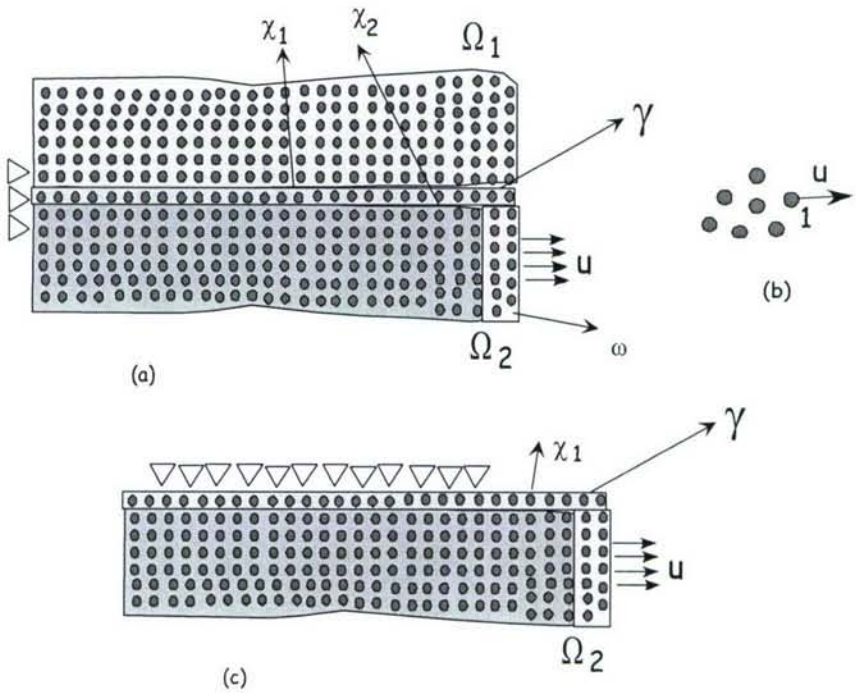

Figure 2. Atomic description of interface

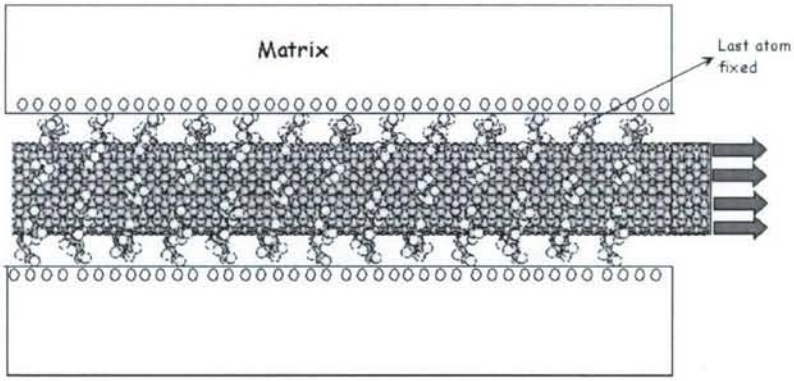

Figure 3. Schematic of the boundary conditions applied in the pullout test simulation

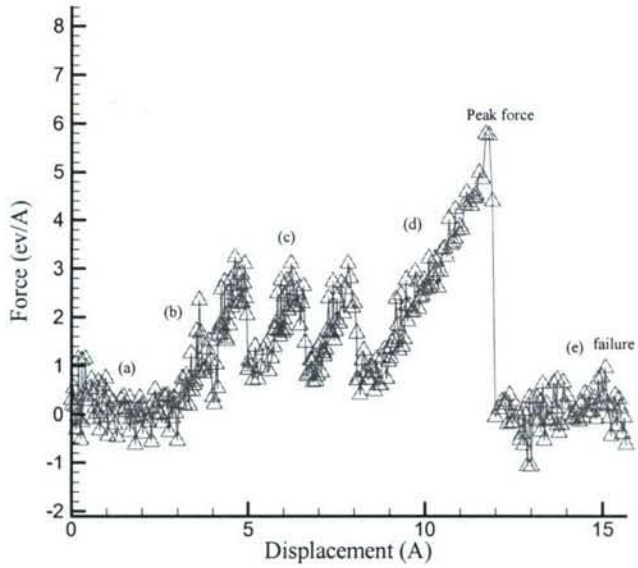

Figure 4. Reaction-force vs displacement for a typical hydrocarbon attachment

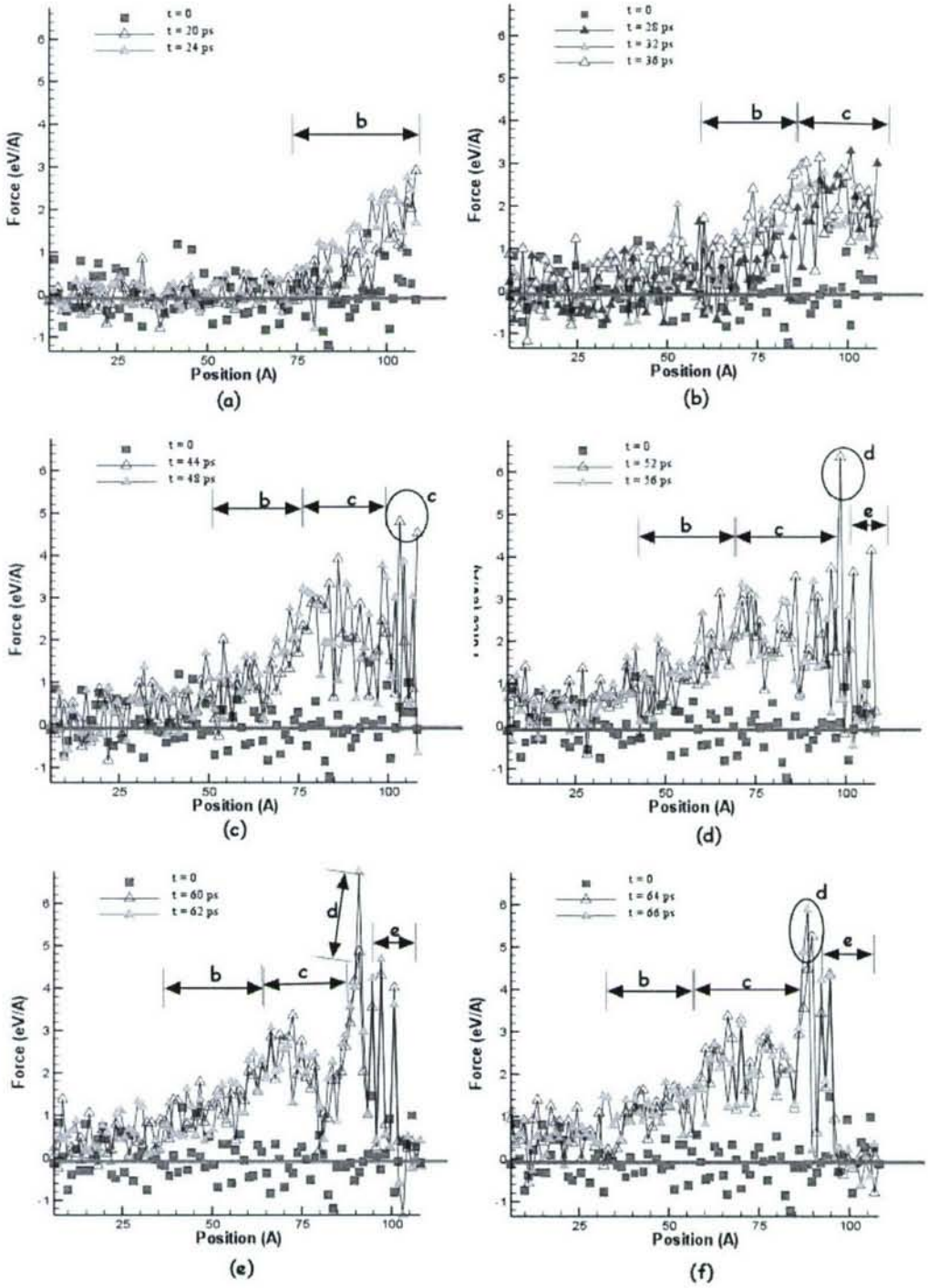

Figure 5. Variation of the reaction force along the length of (10,10) CNT with eighty five chemical attachments at different simulation times

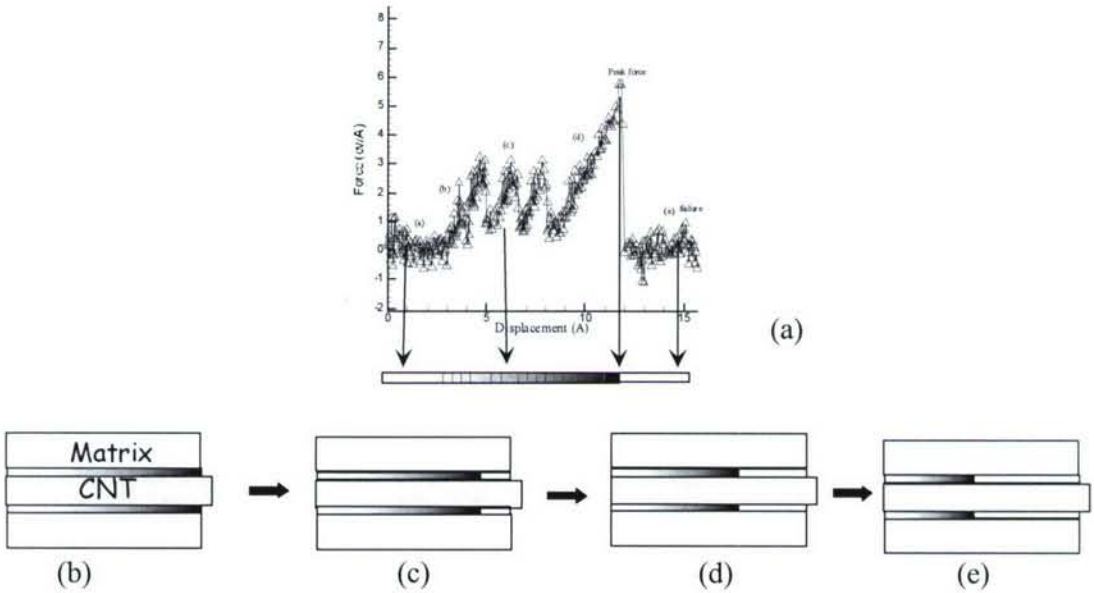

Figure 6. Schematic showing the variation of reaction force with time evolution.

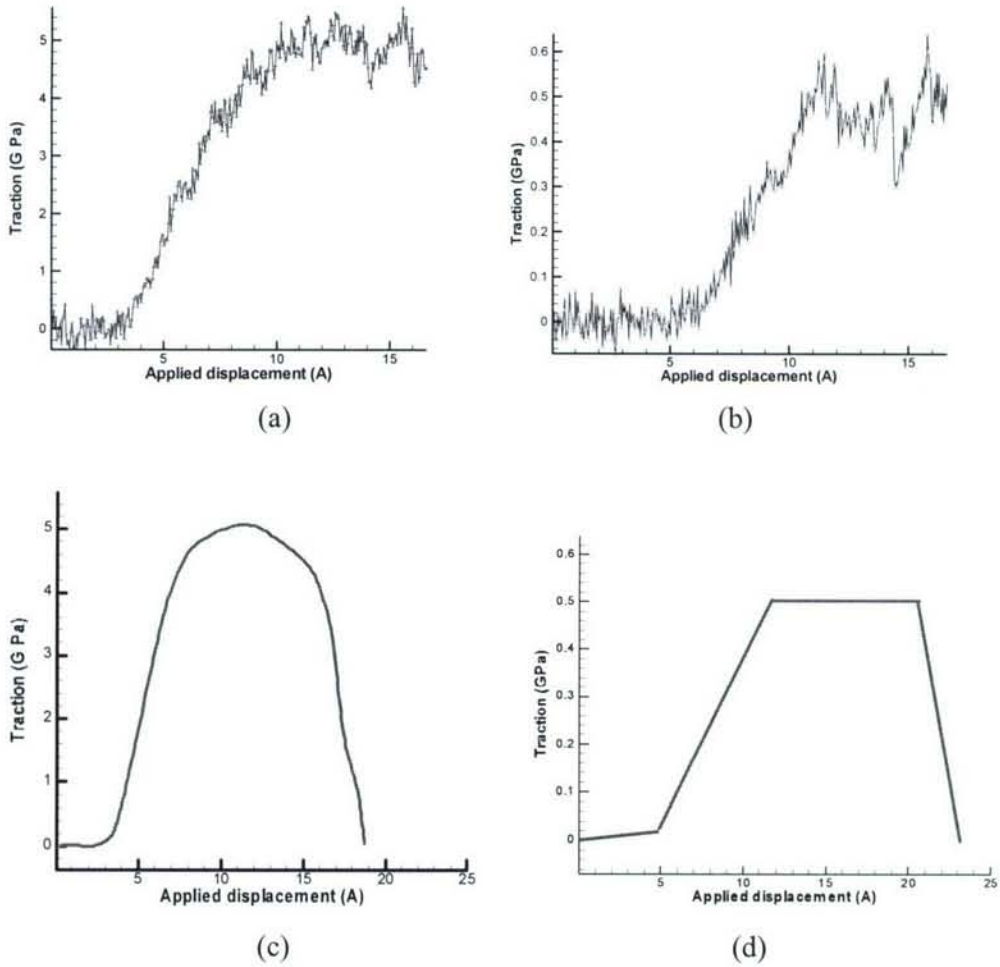

Figure 7. Traction-displacement plots obtained from atomic simulation are shown in (a) and (b). These are extrapolated to obtain the cohesive zone traction displacement relations as in figures (c) and (d)

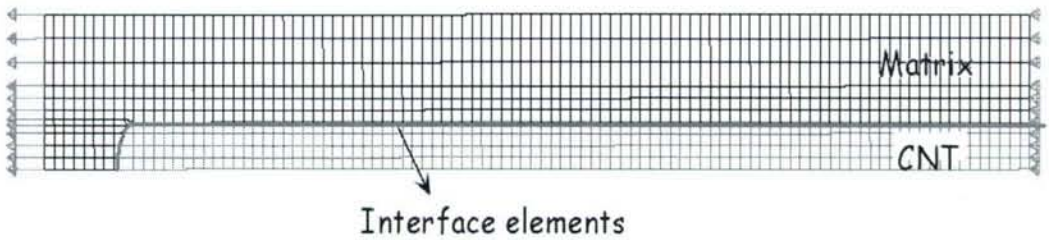

Figure 8. Typical mesh used in the finite element simulations

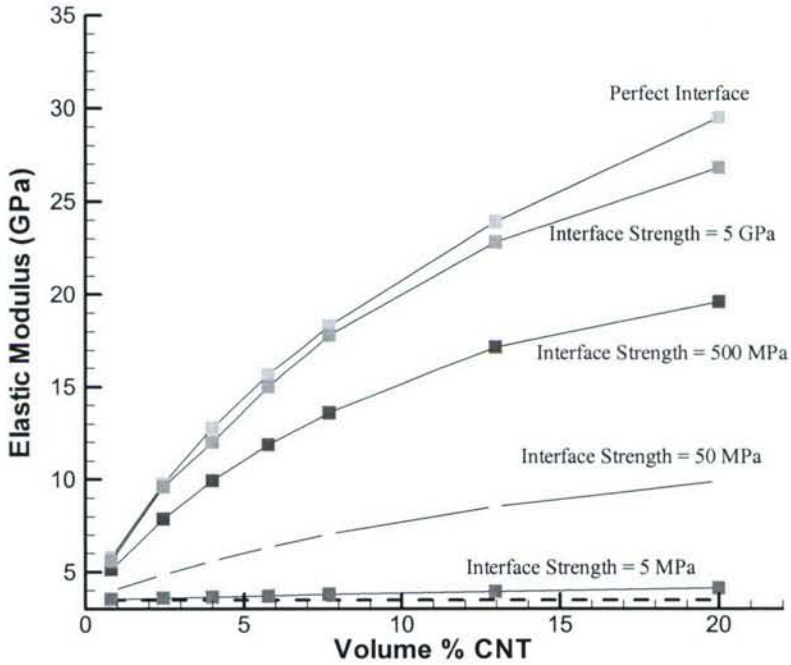

Figure 9. Variation of composite Young's modulus with volume % CNT for different interfacial strengths.

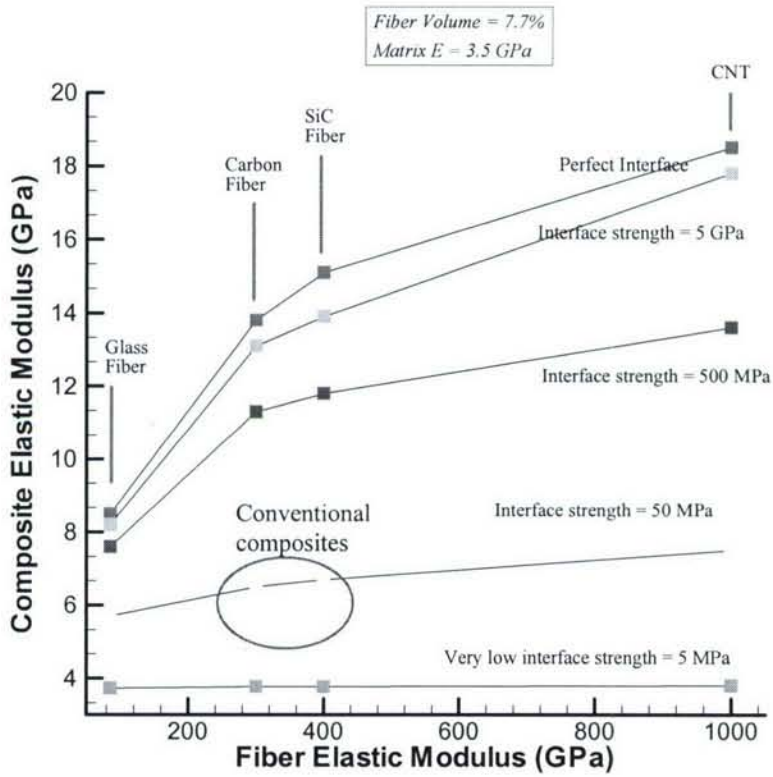

Figure 10. Variation of composite Young's modulus with fiber stiffness for different interfacial strengths.

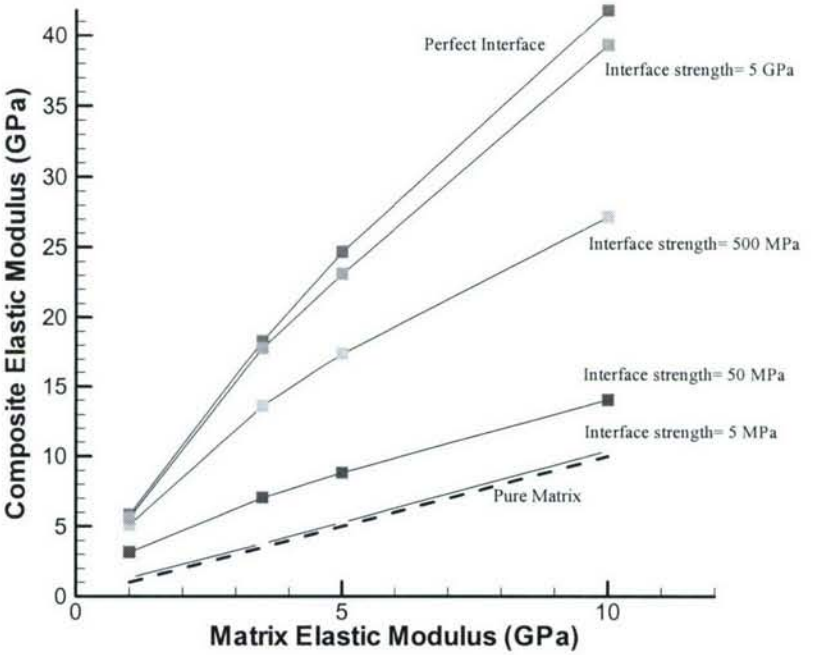

Figure11. Variation of composite Young's modulus with matrix stiffness for different interfacial strengths.